

Experimental insight into the particle morphology changes associated with landslide movement

L. Zuo¹, S.D.N. Lourenco^{2,#}, B.A. Baudet³

¹Department of Civil Engineering, School of Human Settlements and Civil Engineering, Xi'an Jiaotong University, Xi'an, China; formerly The University of Hong Kong

²Department of Civil Engineering, The University of Hong Kong, Hong Kong

³Department of Civil, Environmental and Geomatic Engineering, University College London, UK

[#]Corresponding author

Abstract

Rainfall-induced landslides are major natural hazards that are inherently inter-disciplinary crossing various fields (from geology to hydrology) and scales (particle level to catchment scale and beyond). Comparatively, very few studies on landslides have been conducted at the particle level with most research focusing on particle breakage or the effect of particle size and shape on the macro-scale and particle contact behaviour. Limited evidence suggests that soils under shear undergo changes not only of size, but also of shape and surface roughness. However, the particle morphology descriptors used are frequently qualitative so that information on how the soil particles are damaged during landsliding remains incomplete. This paper uses quantitative particle morphology descriptors, namely particle size, shape and particle surface roughness to investigate particle damage during landslide-induced shearing. A series of ring shear tests were conducted to simulate landslide movement in completely decomposed volcanic rocks (CDV), a typical soil in Hong Kong that was retrieved from a debris flow. Particle size, shape and surface roughness were analyzed on original CDV particles and on samples subjected to ring shear testing. Owing to the crushable nature of the soil, particle breakage was the key factor controlling particle morphology, with the results revealing an intricate dependency of shape and surface roughness on particle size. Shearing enhanced the bimodal gradation of the soil, with the larger grains more rounded and smoother and the resulting fines with a more irregular shape. This may be attributed to a combination of chipping and abrasion of the coarser particles. Further research is needed to ascertain the effect of such particle morphology changes to landslide movement.

Keywords

Debris flows, ring shear test, completely decomposed volcanic rocks, particle

morphology

1. Introduction

Landslides are a major natural hazard at the global scale, with the overexploitation of natural resources, growing urbanization and extreme weather events all contributing to a rise in their frequency (Nadim et al., 2006). During their downslope movement, particles interact by colliding, rolling or sliding past each other. In clays, platelets tend to realign parallel to the shear surface after large shear displacements (Skempton, 1985). In granular materials, particle breakage has been identified at the shear surface of landslides, a phenomenon producing low-permeability layers that generate excess pore water pressure and enhance landslide mobility (Wafid et al., 2004). However, particle breakage is generally accompanied by changes in particle size and shape (e.g. Zhang et al., 2017).

Studies of the evolution of particle morphology during large displacement of granular materials tend to be on rock avalanches (strurzstorms), or in the wind and river dynamics literature. For example, wind erosion produces fines as a result of spalling, chipping and breakage of particles, in a process that includes the removal of particle coatings (Bullard et al., 2004). Kuenen (1960) also found positive relationships between rates of aeolian abrasion and increasing particle size, angularity and surface roughness. In large rock avalanches, particle dynamic fragmentation usually occurs because of the high input energy, and there is evidence that the degree of breakage influences the runout length (Bowman et al., 2012; Bowman & Take, 2015). In submarine landslides however, the processes differ: a recent study of the Nankai Trough (South of Japan) submarine landslide, which was triggered by an earthquake, showed that the seabed particle morphology was barely affected during the movement of the soil. The silty sediments moved down a gentle slope over long travel distances without any noticeable change of the particle size or shape (Li et al., 2018). Morphometric changes to soil particles during landslide events are thus difficult to predict. For instance and for comparison purposes, sandy materials, which are widely distributed in landslide prone regions in South-East Asia, have been less researched than rock avalanches or submarine landslides. Therefore, this paper aims to investigate the evolution of particle morphology in debris flows of sandy materials, by documenting the changes of their size and shape in laboratory-controlled long distance shear tests.

The ring shear apparatus allows unlimited deformation of the specimen tested. Thus, it is often used to simulate and investigate the shearing behaviour of long distance shearing geological phenomenon, such as, for instance, landslides, debris flows and

glacier movements (e.g., Sassa et al., 1996, 2004, 2007; Fukuoka et al., 2007; Iverson et al., 2010; Iverson et al., 1998; Hooyer et al., 2008). Sassa et al. (2004) developed an undrained dynamic-loading ring shear apparatus to simulate the formation of shear zone in rapid landslides. Iverson et al. (2010) performed ring shear tests with a naturally aggregated soil and reported that the post-dilative contraction of aggregates may facilitate debris flow mobilization, while Hooyer et al. (2008) sheared tills to different strain levels with a ring shear apparatus to investigate the fabric evolution during a glacier flow.

The particle characteristics in the shear zone, such as particle size, shape and surface roughness, have been examined with the particle breakage reported as a key factor controlling the shear behaviour (e.g., Coop et al., 2004; Sassa et al., 2004; Zhang et al., 2017). Coop et al. (2004) reported that uniform sands can reach an ultimate fractal grading due to particle breakage when sheared to very large strains. Altuhafi and Baudet (2011) also suggested that natural glacial tills may have reached an ultimate grading *in situ*, while Zhang et al. (2017) found that gap-graded soils retain a memory of their initial grading even at large shearing strains. As for changes to the particle morphology due to breakage, more irregular shapes were reported for the newly created small particles (Altuhafi and Coop, 2011; Zhang et al., 2017), and the particle roughness was shown to be related to the amount of breakage (Altuhafi and Baudet, 2011; Altuhafi and Coop, 2011). Particle breakage modes have also been investigated with single particle crushing tests (e.g., Nakata et al., 1999; Wang and Coop, 2016), with four main modes documented: abrasion and chipping (shallow), and splitting and explosive mode (involving the whole particles). The breakage modes are influenced by the initial particle morphology, mineralogy (Zhao et al., 2015), local shape (roundness) at the particle contacts (Wang and Coop, 2016; Cavarretta et al., 2017), and the initial grading and particle size of the soil (Nakata et al., 1999, 2001).

The importance of particle morphology has also been recognized by numerical modelling who have considered the solid-solid or fluid-solid interaction of particles (e.g. George and Iverson, 2014; Mead and Cleary, 2015; Jing et al., 2016). By means of the Discrete Element Method (DEM), Rait et al. (2012) confirmed that the dynamic fragmentation is indeed important to the spreading behaviour of rock avalanches. Mead and Cleary (2015) found that predictions of mass flow are sensitive to the particle shape and friction values, with the sensitivity to friction highly dependent on the particle shape. It has also been reported that, in general, particle shape plays a significant role in the mechanical behaviour of soils, for example more angular soils have a looser packing and higher compressibility (e.g. Cho et al., 2006; Cavarretta et

al., 2010). The roughness of particle surfaces has also been shown to influence the inter-particle friction (Cavarretta et al., 2010), which is an important parameter to the shear behaviour, but information on the particle surface roughness of real soils are still limited (e.g. Yang et al., 2016).

This paper provides an insight on the magnitude of change of particle size, shape and surface roughness of complete decomposed volcanic rocks (CDV) subjected to shear, which are crushable soils widely occurring in Hong Kong and often existing on steep slopes prone to landslides. The tested CDV was collected from the deposits of a debris flow, analyzed and sheared to large strains by means of a ring shear apparatus. The consequent changes in the particle size, shape and surface roughness within the shear zone were determined. Possible relationships between breakage modes and the evolution of particle size, shape and roughness are also presented.

2. Materials and testing

2.1 Materials

In May 2016, a rainfall-induced debris flow occurred at Sai Wan Road, Sai Kung, Hong Kong (Figure 1). It initiated on a slope angle of about 40° and travelled a distance of 500m down the hillside with a source volume of about 2100m³. The basal failure surface had a maximum depth of about 12m (Geotechnical Engineering Office, 2017). The underlying geology of the area comprises the Long Harbour volcanic formation, which is made of coarse ash tuff and was formed in the Cretaceous period with an approximate age of 142 Ma (Rocchi, 2014). The parent tuff rocks mineralogy is composed of quartz, feldspar, biotite and other mafic and felsic minerals. Chemical weathering degrades the parent rock leading to the decay of all minerals, except quartz, and leads to the formation of new materials such as clay minerals, thus the highly weathered soils contains quartz, feldspar and large amount of clay minerals such as kaolinite, illite and montmorillonite (Okewale & Coop, 2017), which in turn enhances the crushable nature of the soil. The CDV soils were collected from the deposits of the debris flow between 300m and 500m of the runout path, followed by wet sieving to remove the coarser fraction; particles smaller than 2.5mm were kept for further investigation. Scanning Electron Microscopy (SEM) images of CDV particles of different sizes are shown in Figure 2, revealing particles with irregular shapes and rough surfaces. Some cracks can also be observed, indicating that breakage may have occurred during travel. The elemental composition of the CDV particles is shown in Table 1, revealing that the CDV is dominated by silicates. The presence of K, Fe and

Al is typical of these soils and may reflect the chemical weathering the soil has been subjected to.

2.2 Ring shear tests

The ring shear tests were conducted in an apparatus manufactured by Wille Geotechnik (Göttingen, Germany). The ring has an outer diameter of 100mm, inner diameter of 50mm, and height of 25mm. The maximum vertical load and shear load it can apply are 10kN and 7.5kN respectively, and the maximum shear speed that can be reached is 200mm/min. In this study, the CDV specimens were consolidated under different normal stresses, namely 100, 200, 300 and 400kPa, after saturation, to enable the study of the effect of stress level on breakage. Samples were sheared to a displacement of 2.5m, which is equivalent to a shear strain of 1000%, at a shear speed of 5mm/min, which was slow enough to ensure drained conditions. The vertical specimen displacement was also recorded during shearing.

2.3 Determination of particle size and shape

The soils before and after shearing were first sieved into different size ranges, followed by the determination of the particle size and shape with a dynamic image analyzer (Qicpic–Sympatec, Clausthal-Zellerfeld, Germany). Particles larger than 63 μ m were tested with the dry method (GRADIS), in which the particles were dispersed by a vibratory feeder and falling by gravity in front of a laser beam to allow the particle images to be captured. Particles smaller than 63 μ m were tested by a wet method (LIXELL), in which the particles were dispersed in water and then circulated into the apparatus to capture the images. The minimum Feret diameter (the distance between the two parallel planes restricting the particle perpendicular to that direction) is the particle size. Three particle shape indices were measured for a single particle as illustrated in Figure 3, including aspect ratio, which is defined as the ratio of minimum to maximum Feret diameters; convexity, which is calculated as the ratio of the surface area of the particle to the area of the convex hull surface; and sphericity, which is calculated as the ratio of the equivalent area circle perimeter to the real particle perimeter. For reference purposes, a spherical particle achieves a maximum of 1 for the three parameters.

2.4 Determination of particle surface roughness

Optical interferometry has been used to measure the particle surface roughness (e.g., Altuhafi and Baudet, 2011; Nardelli and Coop, 2016; Yang et al., 2016). Two white light beams, reflected by a mirror and the particle surface respectively, are combined to determine the height of each pixel on the surface, and to generate the surface image. The parameter S_q is used to describe the particle surface roughness, and represents the square root of the arithmetic mean of squared deviation from the mean height value (Equation 1):

$$S_q = \left(\frac{1}{n} \sum_{i=1}^n Z_i^2 \right)^{0.5} \quad (1)$$

where n is the number of pixels, and Z is the deviation at each pixel from the mean height value. In this paper, only the roughness of CDV particles larger than 1.18mm was measured with the interferometer as it is not possible to obtain measurements on smaller size particles. The quality of the surface image is strongly dependent on the intensity of the beam reflected by the particle surface. For CDV particles, the existence of clay minerals and hollows on the particle surface generates invalid pixels. To overcome this challenge, a spatial search for sites without invalid pixels is conducted, where roughness is then measured. For a single particle, the S_q value of a surface of $30 \times 30 \mu\text{m}$ was calculated after removing the particle shape effect (Cavarretta et al., 2010; Altuhafi and Baudet, 2011; Yang et al., 2016). A total of 56 particles before shearing and 121 particles after shearing were randomly selected in total.

3. Results and discussion

3.1 CDV shearing behaviour

Representative ring shear results are illustrated in Figure 4. Figure 4(a) shows that under a certain normal stress, specimens with different initial void ratio e_0 reached the same shear resistance at the end of the tests. All the tested specimens showed contractive behaviour with an immediate decrease in the height at the beginning followed by a quasi-steady state. Residual shear strength obtained under different normal stress levels revealed a friction angle ϕ of 29.7° as shown in Figure 4(b). Okewale & Coop (2017) performed triaxial tests on CDV and reported the critical state angle of shearing resistance to be 31° for the most weathered soils.

3.2 Particle breakage

Both the cumulative and density distributions of the original CDV soil are shown in Figure 5 with red solid lines. It shows that the soil is well-graded with particles ranging from clay to sand size, and more than 60% of the soil is smaller than 63 μm . Silt particles with a size of 20-40 μm and sand particles with a size of 1000-2000 μm are the two main fractions indicated by the peaks of the density distribution, while the lack of particles within 100-500 μm range renders the soil slightly gap-graded. This feature is usually seen in saprolites, which is attributed to the disintegration of the parent rocks (Okewale & Coop, 2017).

The density distributions of the soil particles after shearing are plotted in Figure 5(b). Compared to the original curve, there is a clear reduction in the sand fraction and an increment in the silt fraction. The peak for the sand particles moves down and shifts slightly to the left, while the peak for the silt particles moves up and shifts to the right. This suggests the occurrence of particle breakage within the sand particles during shearing, mainly for the particles larger than 600 μm (a small amount of breakage can still be observed at the particle size of 200 μm). Both the mass by percentage and size of the sand particles decreased due to the breakage. A large amount of small particles were created during shearing, especially within the size range of 30-60 μm , marking an increase in the mean particle size of the silt fraction. This demonstrates that the shearing performed in the ring shear apparatus accentuated the bimodal nature of the particle size distribution, possibly indicating that the breakage that would have occurred during the debris flow also resulted in the same bimodal grading.

The similarity of the density distribution curves after shearing under different normal stresses suggests a high crushing potential of the CDV particles. This potential is also reported by Sandeep and Senetakis (2017). Particles of CDV contain clay minerals, internal voids, impurities and weak mineral boundaries, with breakage more likely to occur within these microstructures (Zhao et al., 2015). A possible explanation for the creation of the large amount of silt sized particles is put forward as follows: during shear sand particles are mainly in contact with silt particles as the initial silt content is high, resulting in a high contact number and relatively low local stresses at particle contacts. These weak microstructures near the sand particle surface could easily be removed by abrasion or chipping, thus generating further fine-sized particles (as exemplified in Figure 6).

3.3 Particle morphology

The distribution of aspect ratio, convexity and sphericity of the original CDV soil against particle size are shown in Table 2 and Figures 7 and 8 in red solid lines. Particles larger than 63 μm (in Figure 7(a)), have a relatively constant aspect ratio equal to 0.75 ± 0.02 . There is however a clear increase in convexity as the particle size increases, from 0.89 to 0.94, indicating a decrease in angularity with size, and a marked decrease in sphericity from 0.90 to 0.84, indicating less circular shapes (Figures 7(b) and 7(c)). Particles smaller than 63 μm , when compared to the sand size particles, have shape factors with lower values, with a mean aspect ratio of about 0.74, mean convexity value of 0.87 and mean sphericity value of 0.85, as shown in Figure 8 and Table 2. These values are closer to what is found, for example, on a standard quartzitic sand such as Leighton Buzzard sand (LBS), which has a mean aspect ratio of 0.76, convexity of 0.96 and sphericity of 0.89 for particle sizes in the range 600-1180 μm . The parent volcanic rock, being the product of rapid cooling lava, would have had relatively small minerals, thus it is expected that the silt size particles of CDV contain minerals such as quartz, but these would have less rounded shapes than a river sand such as LBS which has been transported before deposition. The larger sand size particles of CDV may be agglomerates of coarse and fine soil particles, leading to less spherical particles. Clay size fines may infill the concavities enhancing the overall particle convexity.

The values of the shape factors increase slightly for the particles larger than 63 μm after shearing, especially for the particles larger than 1mm as shown in Figure 7. The aspect ratio seems to be the least sensitive to the particle breakage, since it remains nearly unchanged after shearing, with the largest increment still less than 0.03 for a particle size around 2mm. The convexity and sphericity are more affected over the whole range of particle size, while the increments are still limited. Altuhafi and Baudet (2011) reported that the increase in convexity and sphericity results from the abrasion or chipping of asperities, while the aspect ratio could remain almost unchanged since the particle Feret diameters are less influenced. Although not significant, the changes in sphericity after shearing may suggest a breakage mode of abrasion or chipping (as shown in Figure 6).

For the silt size particles, all the values of the shape factors decrease after shearing as shown in Figure 8. It suggests that the small particles created during particle breakage have even more irregular shapes, which is in agreement with former results (Altuhafi and Baudet, 2011; Altuhafi and Coop, 2011; Zhang et al., 2017). Note that the particle shape differences around 63 μm in Figure 7 and 8 can be attributed to the use of different testing methods, GRADIS (>63 μm) and LIXELL (<63 μm). However, the

particle shape comparison before and after shearing remains unaffected.

3.4 Particle surface roughness

The S_q values of randomly selected particles larger than 1.18mm, before and after shearing, are summarized in Figure 9(a), and the cumulative distribution curves calculated by the particle number are shown in Figure 9(b). The original CDV particles have relatively high S_q values, ranging between 1000 and 1500nm, with an average value of 1206nm and a standard deviation of ± 265 nm. This is two to three times higher than the roughness of documented soil particles. For instance, LBS particles of size 1.18-5mm have been reported to have values of S_q of about 400-600nm (Senetakis et al., 2013; Yang et al., 2016). The rough nature of the surface is visible in Figure 2, and may be indicative of the fines attached to the surface of coarse particles.

Shearing induces a clear reduction in the S_q value, despite 8 (out of 121) particle surfaces remaining with a comparatively high roughness as shown in Figure 9(a). This may indicate that these particles were not affected by shearing, as suggested by the particle size distribution showing that some large particles remain intact even after shearing. Most of the tested particles (95 out of 121) have a S_q value after shearing within 700-1200nm, and the average and standard deviation values are 919 (± 270), 967 (± 277), 876 (± 143), 982 (± 269) nm, for the normal stresses of 100, 200, 300, 400kPa, respectively. Some surfaces have a S_q value below 500nm, which was not observed for the original CDV particles. To illustrate the meaning of the different S_q values, Figure 10 shows random 3D images of surfaces with different roughness and corresponding cross-section profiles. A clear irregular profile can be observed for the rougher surface, which becomes less significant as the surface becomes smoother.

Two types of surface topography created by shearing can be observed in the SEM images shown in Figure 11. Figure 11(a) shows particles with chipped surfaces that are likely to have developed during shear. It can be observed that the newly created surface still has an irregular shape but is smoother compared to the original one, thus the surface roughness is lowered although part of the surface remains rough. Figure 11(b) shows particles with a clear geometric shape. The particle, which is assumed to be quartz due to its hexagonal shape, was originally coated by other particles; while after shearing, the surfaces were uncoated by abrasion. This justifies the existence of surfaces with a S_q value below 500nm, which is close to values found for quartz particles (such as LBS particles).

3.5 Implications for landslide mechanics

We can attempt to draw parallels between the evolution of the size and shape distribution during shearing in the ring shear apparatus, and how they might have evolved during the debris flow. Mechanical weathering of the volcanic parent rock may have led to fracturing of the initial structure into coarse agglomerates made of coarse particles amalgamated with a finer matrix. Further weathering would have caused asperities to break and fines to detach, creating a gap-graded to well-graded particle size distribution. Further damage by the landslide movement could exacerbate the phenomenon, as was observed in the grading of the original CDV retrieved from the debris flow and confirmed by the results of the ring shear tests. This is accompanied by evidence from their shape that the smaller particles may be representative of quartz, which is hidden in the larger particle sizes by the amalgamation of fines. An investigation of the roughness of the particle surface of the two different sizes could shed more light.

Particle breakage has been suggested to influence landslide mobility. In rock avalanches, the initially relatively intact rock mass undergoes breakage during runout with highly fragmented debris created and spread at high speed (Dufresne and Dunning, 2017). Field observations also suggest that the deposits of rapid landslides (e.g. debris avalanches) show the ubiquitous characteristic that a major portion of their material has been highly fragmented to various degrees during travel (Jiang et al., 2016). Davies and McSaveney (2009) proposed that stored elastic strain energy can be released during particle fragmentation, with the transient elastic energy generating an isotropic dispersive stress which supports the overburden and decreases the effective stress in the particle flow. This leads to an overall reduction in the shear resistance that enhances landslide mobility. However, by performing fast ring shear tests on dry silica sand, Jiang et al. (2016) reported that the energy released by particle crushing was insufficient to decrease the shear resistance despite a large amount of breakage occurring. For the crushable CDV material used in the presented paper, breakage develops near the particle surface by means of abrasion or chipping, possibly releasing comparatively less energy than silica sand. Thus, and without accounting for particle shape and surface roughness effects, particle breakage of fine materials (sand and smaller) is less likely to contribute to landslide mobility than a fragmented rock mass (boulders and larger) would.

4. Conclusions

By using an experimental methodology approach that combines quantitative measurements of particle size, shape and surface roughness of a well graded, crushable CDV soil collected from a debris flow deposit in Hong Kong, an insight into the mechanisms controlling the particle damage during movement has been made possible. Analysis of the particle sizes revealed a bimodal distribution, while image analysis of the particle shape and roughness showed that the coarser sand size fraction was most probably formed of agglomerates of coarse and fine particles, while the finer silt size fraction contained more discrete mineral particles such as quartz.

Ring shear tests were conducted on the same material (CDV) under drained condition and revealed a residual friction angle ϕ of 29.7° . The particle size, shape and surface roughness were compared before and after shearing. A clear reduction in the coarser sand fraction and an increment in the silt fraction were found after shearing, indicating a high crushing potential of the larger CDV particles. Shearing in the ring shear apparatus confirmed the bimodal trend seen on the original CDV retrieved from the deposition zone. The breakage mode is assumed to be abrasion or chipping due to the high silt content. The original CDV particles have an irregular shape. After shearing, the sand particles become slightly rounded, while the newly created silt particles have a more irregular shape. The sphericity is more sensitive to breakage than the aspect ratio, again suggesting a breakage mode of abrasion or chipping. A reduction of particle surface roughness was also observed. The original CDV particles have relatively rough surfaces; while after shearing, surface roughness reduces due to the creation of chipped surface or uncoated quartz surface by abrasion or chipping.

The ring shear tests results suggest that the debris flow in this particularly crushable soil may have caused the fragmentation of coarse, agglomerate particles with abrasion taking place during the rolling and sliding. The fines generated by the abrasion may have in turn maintained the flow behaviour, with the coarse particles being enclosed in a matrix of smoother, finer particles. On the other hand, comparing to the fragmentation of a rock mass, the energy released by the breakage of crushable CDV particles is insufficient and contributes less to the debris flow mobility.

Acknowledgements

The authors acknowledge the financial support provided by the General Research Fund, Research Grants Council, Hong Kong (17200114, T22-603/15-N), and by the State Key Laboratory of Geo-hazard Prevention and Geo-environmental Protection of

the University of Technology, Chengdu. The authors are very grateful to Professor Wei Hu for facilitating the use of the ring shear apparatus in his laboratory. We also acknowledge the Head of the Geotechnical Engineering Office and the Director of the Civil Engineering and Development, the Government of the Hong Kong Special Administrative Region, for the permission to publish the photograph in Figure 1.

References

- Altuhafi FN, Baudet BA (2011) A hypothesis on the relative roles of crushing and abrasion in the mechanical genesis of a glacial sediment. *Eng Geol* 120:1-9
- Altuhafi FN, Coop MR (2011) Changes to particle characteristics associated with the compression of sands. *Géotechnique* 61(6):459-471
- Bowman ET, Take WA, Rait AL, Hann C (2012) Physical models of rock avalanche spreading behaviour with dynamic fragmentation. *Can Geotech J* 49(4):460-476
- Bowman ET, Take WA (2015) The runout of chalk cliff collapses in England and France—case studies and physical model experiments. *Landslides* 12:225-239
- Bullard JE, Mctainsh GH, Pudmenzky C (2004) Aeolian abrasion and modes of fine particle production from natural red dune sands: an experimental study. *Sedimentology* 51:1103-1125
- Cavarretta I, Coop MR, O’Sullivan C (2010) The influence of particle characteristics on the behaviour of coarse grained soils. *Géotechnique* 60(6):413-423
- Cavarretta I, O’Sullivan C, Coop MR (2017) The relevance of roundness to the crushing strength of granular materials. *Géotechnique* 67(4):301-312
- Cho GC, Dodds JS, Santamarina, JC (2006) Particle shape effects on packing density, stiffness, and strength: natural and crushed sands. *J Geotech Geoenviron* 132(5):591-602
- Coop MR, Sorensen KK, Bodas Freitas T, Georgoutsos G (2004) Particle breakage during shearing of a carbonate sand. *Géotechnique* 54(3):157-163
- Davies TRH, McSaveney MJ (2009) The role of rock fragmentation in the motion of large landslides. *Eng Geol* 109:67-79
- Dufresne A, Dunning SA (2017) Process dependence of grain size distributions in rock avalanche deposits. *Landslides* 14:1555-1563
- Fukuoka H, Sassa K, Wang G (2007) Influence of shear speed and normal stress on the shear behavior and shear zone structure of granular materials in naturally drained ring shear tests. *Landslides* 4:63-74
- Geotechnical Engineering Office (2017) Summary of findings of landslide investigation. Civil Engineering and Development Department Website. http://hkss.cedd.gov.hk/hkss/eng/lic/Html_16/saiwanroad.aspx. Accessed 10 November 2018.
- George DL, Iverson RM (2014) A depth-averaged debris-flow model that includes the effects of evolving dilatancy. II. Numerical predictions and experimental tests. *P R Soc A* 470:20130820
- Hooyer TS, Iverson NR, Lacroix F, Thomason JF (2008) Magnetic fabric of sheared till: A strain indicator for evaluating the bed deformation model of glacier flow. *J*

- Geophys Res-Earth 113, F02002
- Iverson NR, Hooyer TS, Baker RW (1998) Ring-shear studies of till deformation: Coulomb-plastic behavior and distributed strain in glacier beds. *J Glaciol* 44:634-642
- Iverson NR, Mann JE, Iverson RM (2010) Effects of soil aggregates on debris-flow mobilization: Results from ring-shear experiments. *Eng Geol* 114:84-92
- Jiang Y, Wang G, Kamai T (2017) Fast shear behavior of granular materials in ring-shear tests and implications for rapid landslides. *Acta Geotech* 12(3):645-655
- Jing L, Kwok CY, Leung YF, Sobral YD (2016) Extended CFD-DEM for free-surface flow with multi-size granules. *Int J Numer Anal Met* 40:62-79
- Kuenen PH (1960) Experimental abrasion 4: eolian action. *J Geol* 68: 427-449
- Li SKM, Zuo L, Nardelli V, Alves T, Lourenco SDN (2018) Morphometric signature of sediment particles reveals the source and emplacement mechanisms of submarine landslides. *Landslides* (under review)
- Mead SR, Cleary PW (2015) Validation of DEM prediction for granular avalanches on irregular terrain. *J Geophys Res-Earth* 120:1724-1742
- Nadim F, Kjekstad O, Peduzzi P, Herold C, Jaedicke C (2006) Global landslide and avalanche hotspots. *Landslides* 3:159-173
- Nakata Y, Hyde AFL, Hyodo M, Murata H (1999) A probabilistic approach to sand particle crushing in triaxial test. *Géotechnique* 49(5):567-583
- Nakata Y, Hyodo M, Hyde AFL, Kato Y, Murata H (2001) Microscopic particle crushing of sand subjected to high pressure one-dimensional compression. *Soils Found* 41(1):69-82
- Nardelli V, Coop MR (2016) The micromechanical behaviour of a biogenic carbonate sand. *Procedia Engineer* 158:39-44
- Okewale IA, Coop MR (2017) A study of the effects of weathering on soils derived from decomposed volcanic rocks. *Eng Geol* 222:53-71
- Rait KL, Bowman ET, Lambert C (2012) Dynamic fragmentation of rock clasts under normal compression in sturzstrom. *Geotech Lett* 2(3):167-172
- Rocchi I (2014) An experimental investigation of the influence of weathering on saprolitic soils from Hong Kong. Dissertation, City University of Hong Kong
- Sandeep CS, Senetakis K (2017) Exploring the micromechanical sliding behaviour of typical quartz grains and completely decomposed volcanic granules subjected to repeating shearing. *Energies* 10(3):370
- Sassa K, Fukuoka H, Scarascia-Mugnozza G, Evans S (1996) Earthquake-induced-landslides: distribution, motion and mechanisms. *Soils Found*, Special Issue for the Great Hanshin Earthquake Disaster, pp 53-64

- Sassa K, Fukuoka H, Wang G, Ishikawa N (2004) Undrained dynamic-loading ring-shear apparatus and its application to landslide dynamics. *Landslides* 1:7-19
- Sassa K, Fukuoka H, Wang G, Wang F (2007) Undrained stress-controlled dynamic-loading ring-shear test to simulate initiation and post-failure motion of landslides. In: Sassa K, Fukuoka H, Wang F, Wang G (eds) *Progress in Landslides Science*, 1st edn. Springer, Verlag Berlin Heidelberg, pp 81-98
- Senetakis K, Coop MR, Todisco MC (2013) The inter-particle coefficient of friction at the contacts of Leighton Buzzard sand quartz minerals. *Soils Found* 53(5):746-755
- Skempton, AW (1985) Residual strength of clays in landslides, folded strata and the laboratory. *Géotechnique* 35(1):3-18
- Wafid M, Sassa K, Fukuoka H, Wang G (2004) Evolution of shear-zone structure in undrained ring-shear tests. *Landslides* 1:101-112
- Wang W, Coop MR (2016) An investigation of breakage behaviour of single sand particles using a high-speed microscope camera. *Géotechnique* 66(12):984-998
- Yang H, Baudet BA, Yao T (2016) Characterization of the surface roughness of sand particles using an advanced fractal approach. *P R Soc A* 472:20160524
- Zhang X, Baudet BA, Hu W, Xu Q (2017) Characterization of the ultimate particle size distribution of uniform and gap-graded soils. *Soils Found* 57(4):603-618
- Zhao B, Wang J, Coop MR, Viggiani G, Jiang M (2015) An investigation of single sand particle fracture using X-ray micro-tomography. *Géotechnique* 65(8):625-641

Tables and Figures

Table 1 Elemental composition of CDV particles

Elements	Weight (%)	Atomic (%)
O	50.81	58.98
Si	24.23	16.02
C	10.43	16.13
Al	10.42	7.17
Fe	2.32	0.77
K	1.52	0.72
Mg	0.28	0.21

Table 2 Morphological properties of CDV particles before and after shearing

Morphological properties	CDV particles									
	coarse (63~2500 μ m)					fine (<63 μ m)				
	original	normal stress (kPa)				original	normal stress (kPa)			
		100	200	300	400		100	200	300	400
Mean particle size (μ m)	969	823	811	817	825	23	33	47	54	33
Mean aspect ratio	0.76	0.76	0.76	0.75	0.75	0.74	0.72	0.71	0.72	0.71
Mean convexity	0.93	0.93	0.93	0.94	0.94	0.87	0.87	0.87	0.87	0.86
Mean sphericity	0.85	0.85	0.86	0.86	0.86	0.85	0.83	0.82	0.83	0.81
Mean surface roughness* (nm)	1206	919	967	876	982	-	-	-	-	-

*Surface roughness is only measured for particles larger than 1.18mm



Fig. 1 Photograph of the Sai Wan Road, Sai Kung landslide (distance from the crown to the road is 137m)

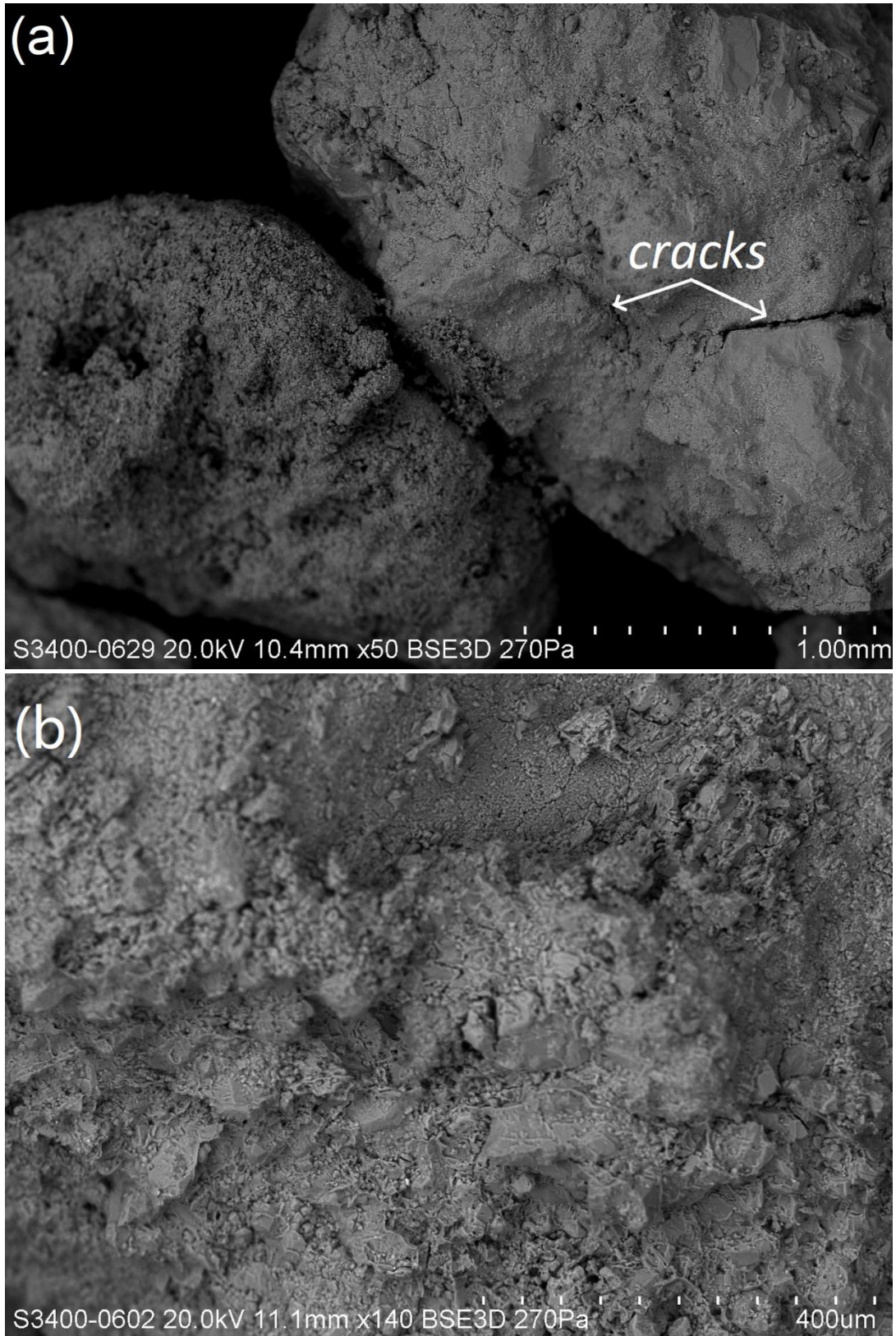


Fig. 2 SEM images of 1.18-2.5mm CDV particles: (a) particle with cracks, (b) rough particle surface

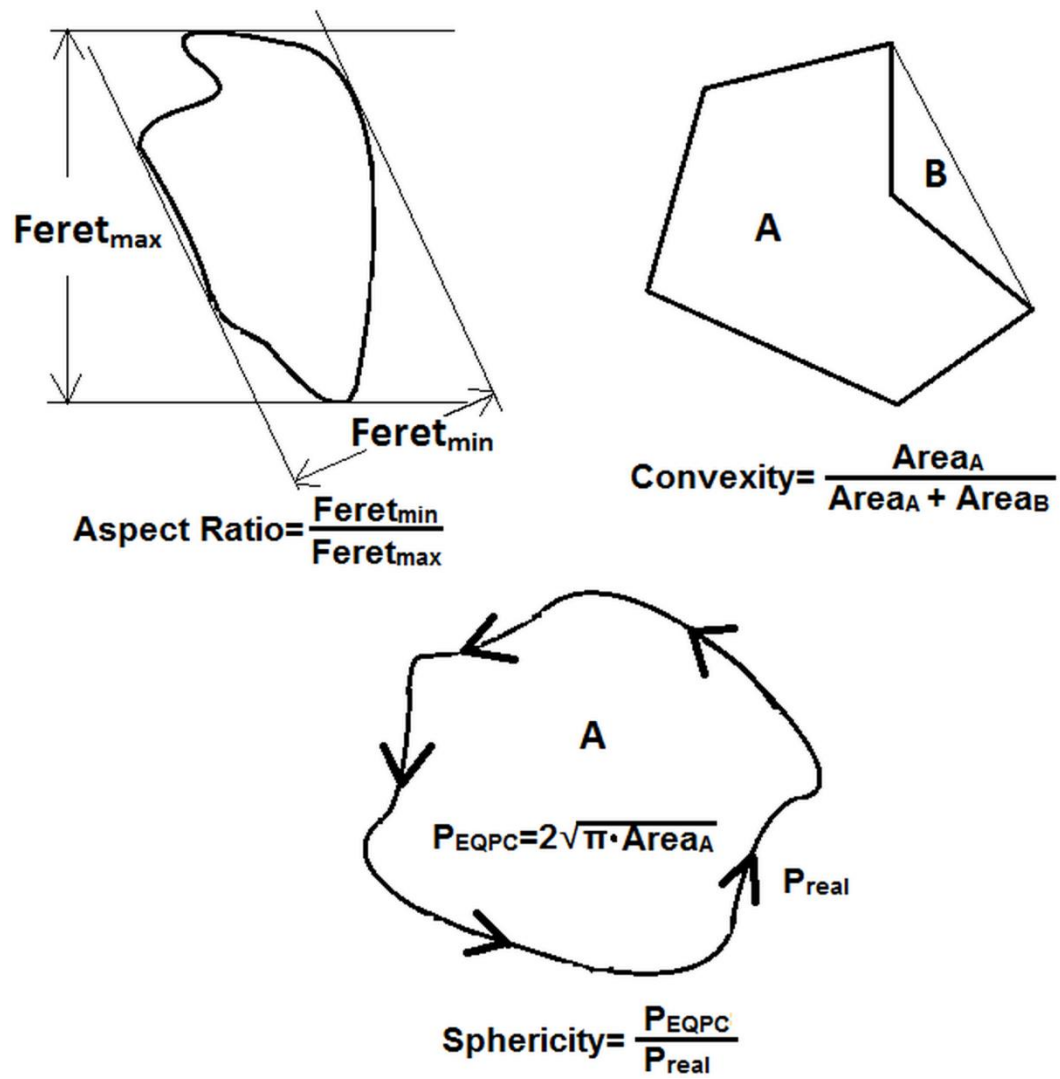


Fig. 3 Schematic diagram of the particle shape indices (aspect ratio, convexity and sphericity)

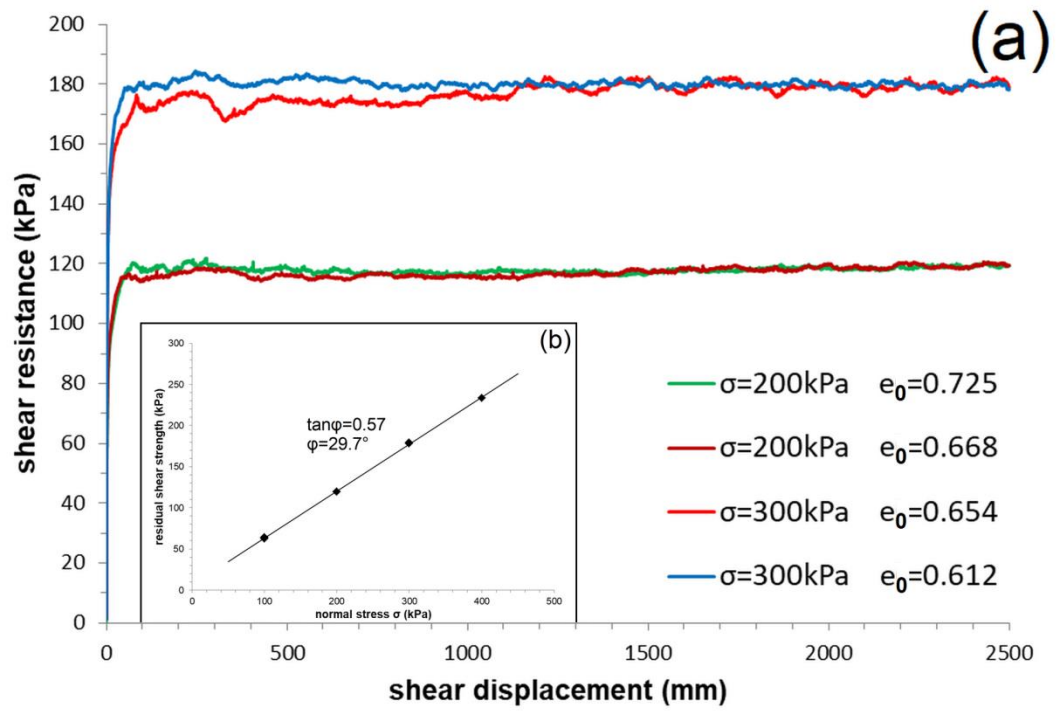


Fig. 4 Ring shear test results for the completed decomposed volcanic soil: (a) development of shear resistance, (b) the residual shear strength under different normal stress levels

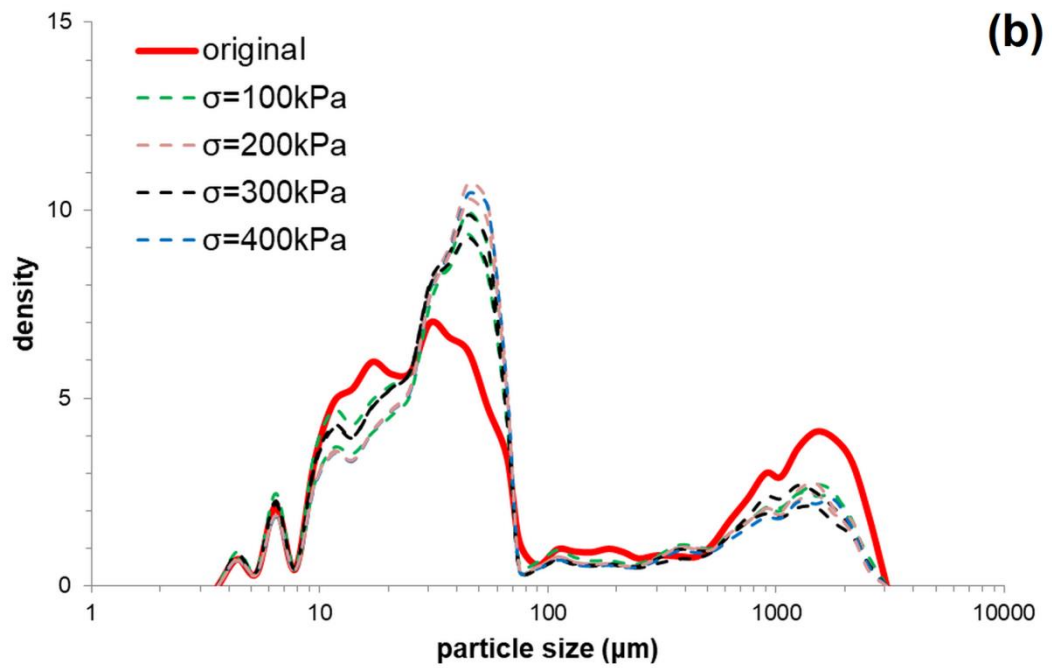
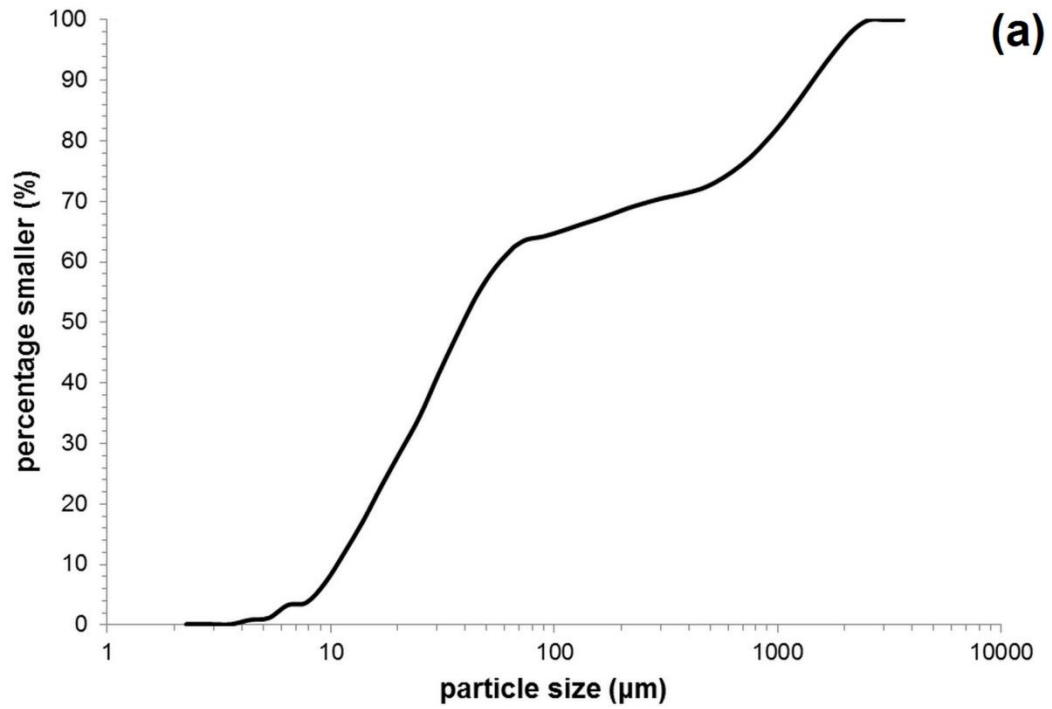


Fig. 5 Particle size distribution of the CDV soil: (a) cumulative distribution of the soil before shearing, (b) density distributions of the soil before and after shearing

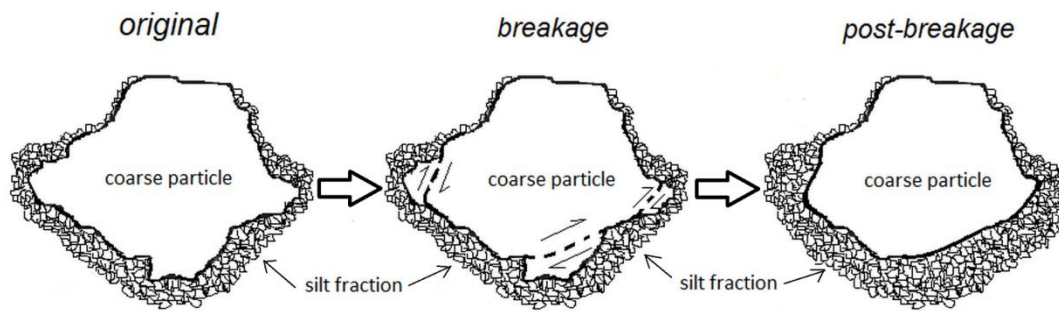
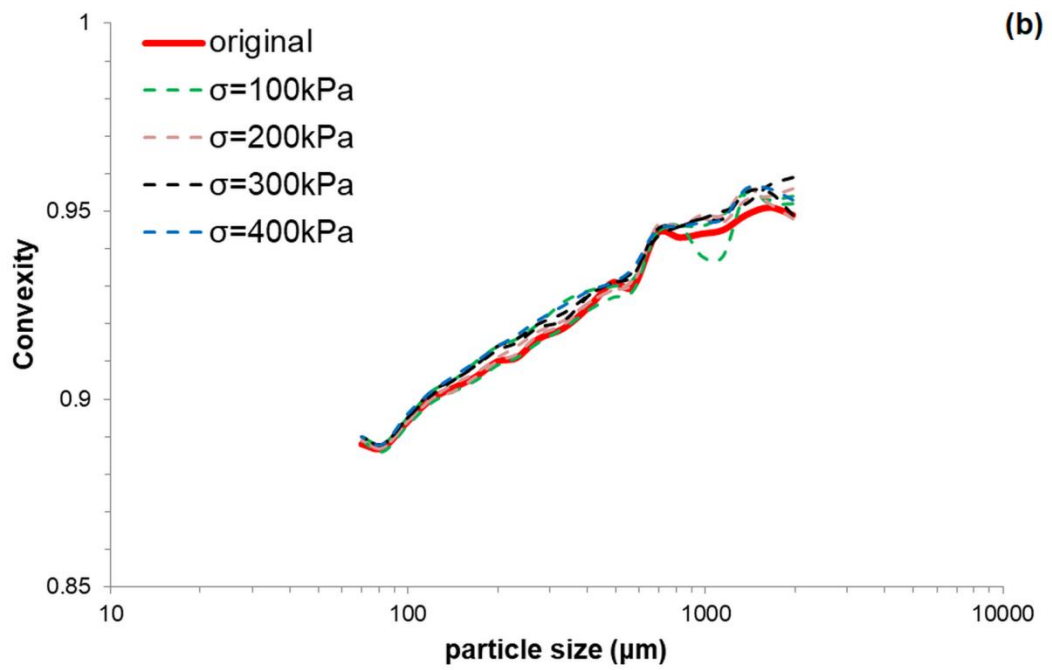
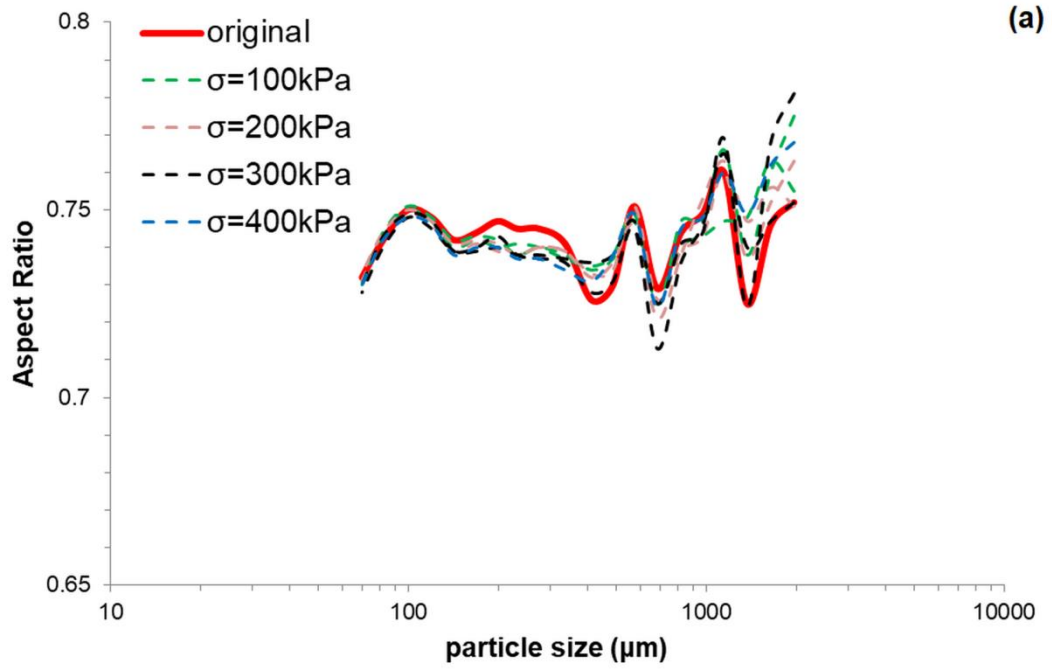


Fig. 6 Conceptual diagram of the particle morphology changes with shearing: silt fraction increases after shearing, coarse fraction becomes slightly more rounded while silt fraction becomes more angular



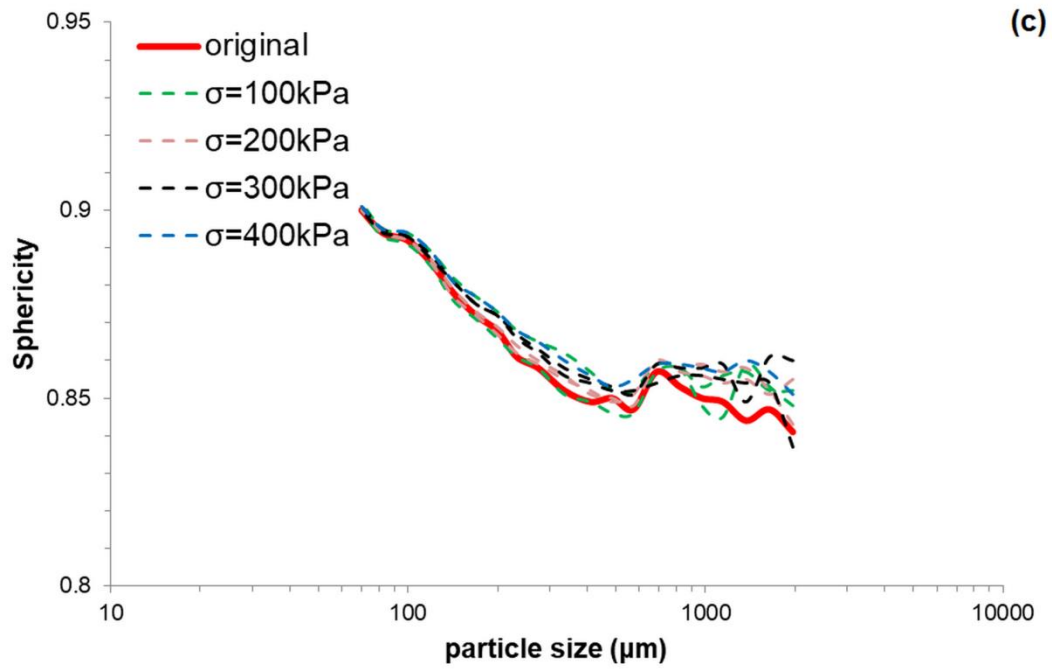
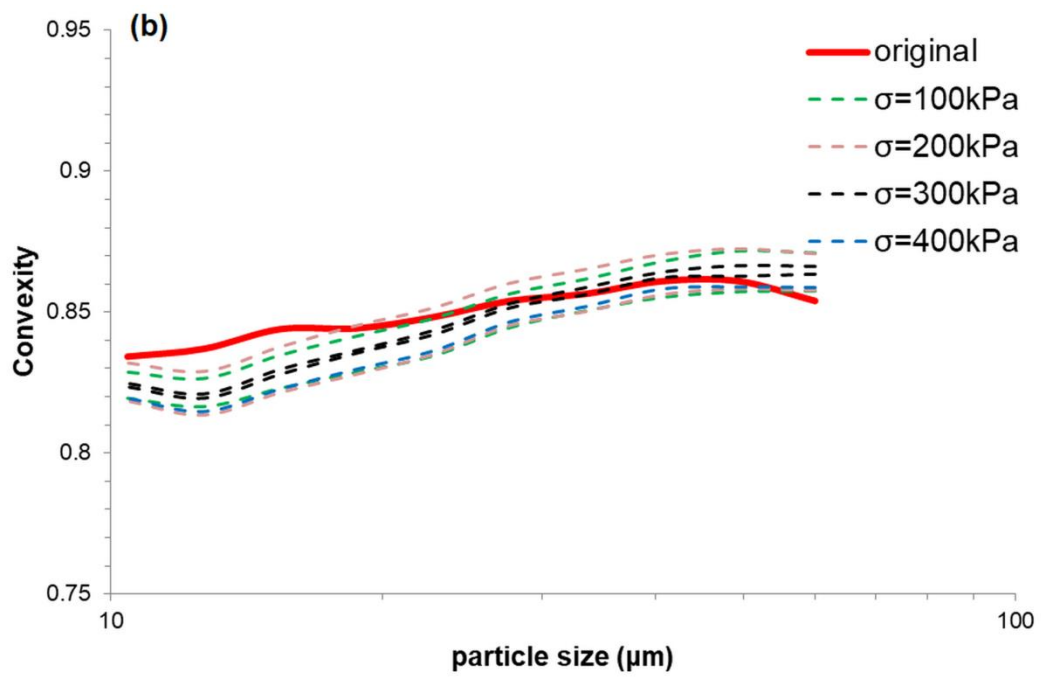
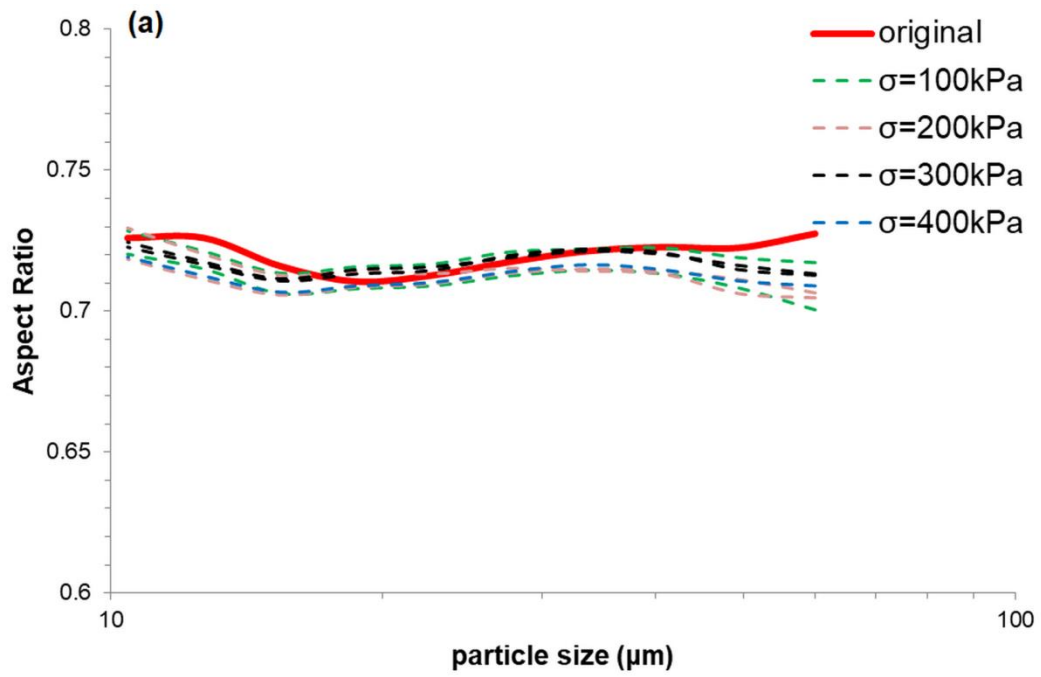


Fig. 7 Variation of the shape factors for the particles larger than 63 μm before and after shearing: (a) aspect ratio, (b) convexity, (c) sphericity



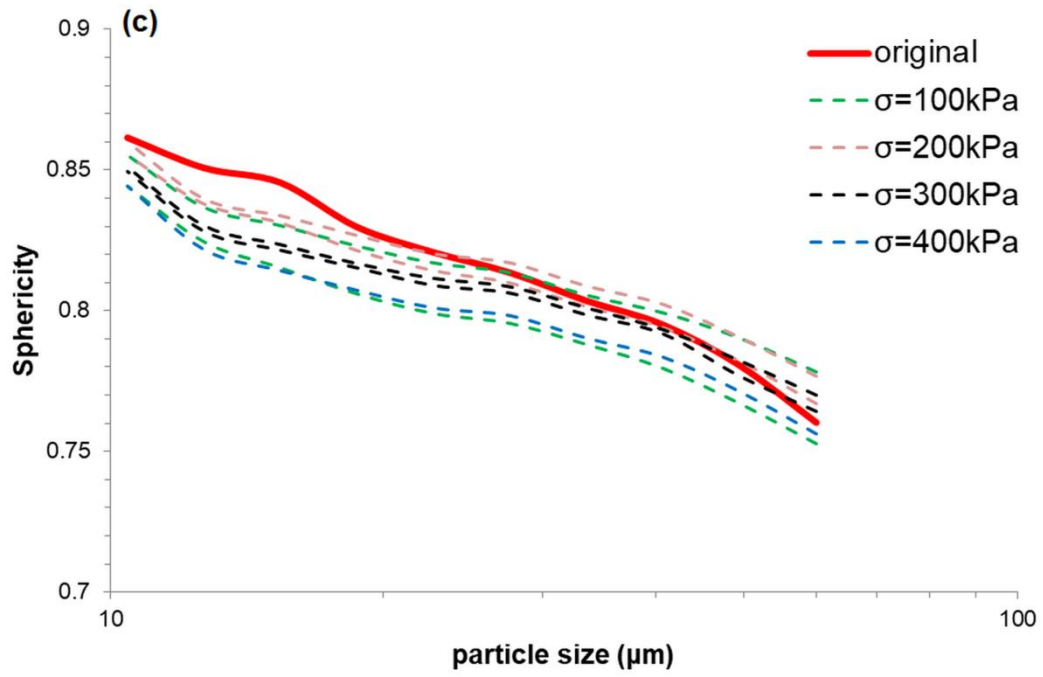


Fig. 8 Variation of the shape factors for the particles smaller than $63\mu\text{m}$ before and after shearing: (a) aspect ratio, (b) convexity, (c) sphericity

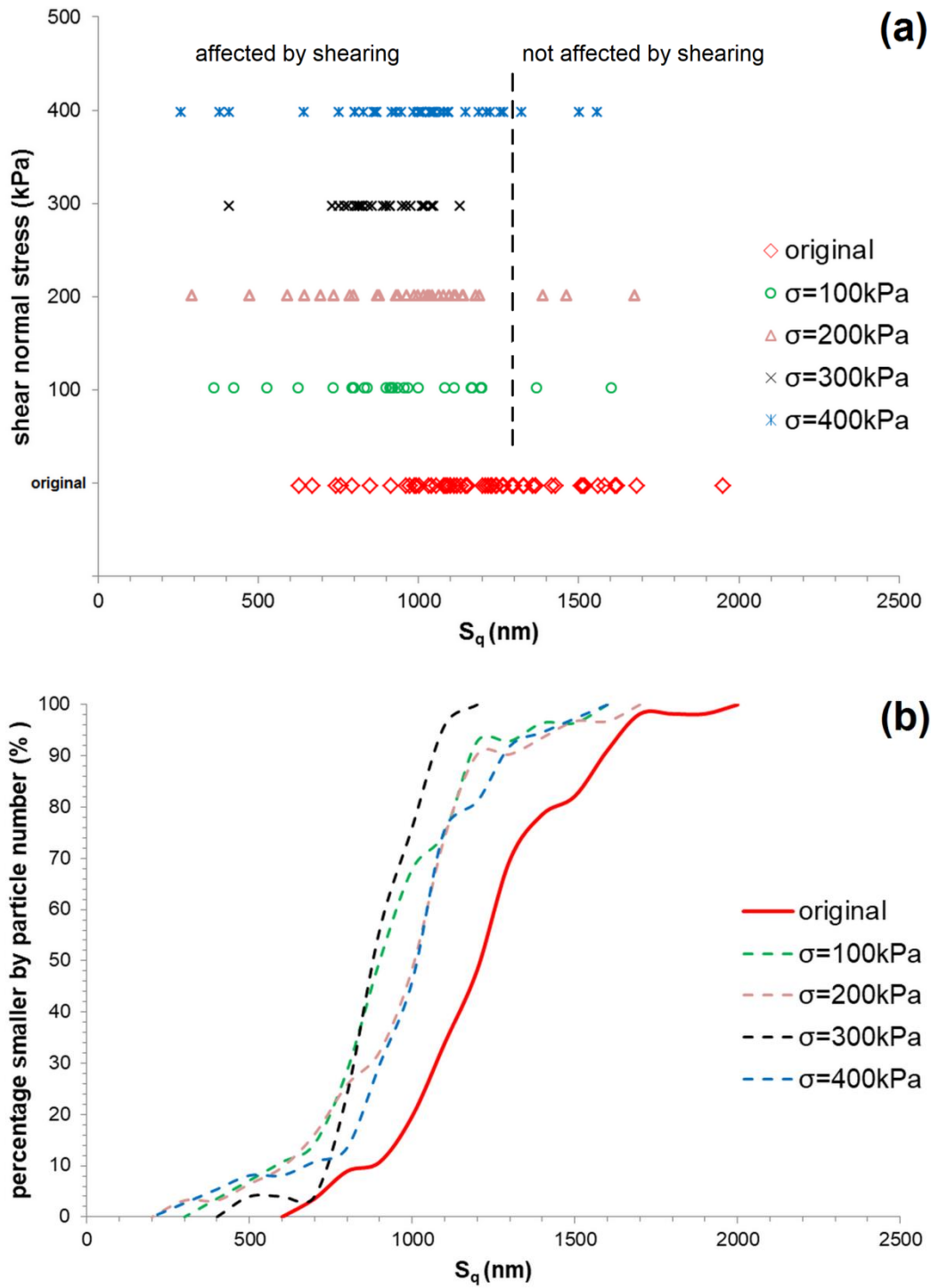


Fig. 9 Surface roughness of CDV particles before and after shearing: **(a)** summary of S_q values (particles to the right-hand side of the vertical dashed line are assumed not to be affected by shearing), **(b)** cumulative distribution calculated by particle numbers

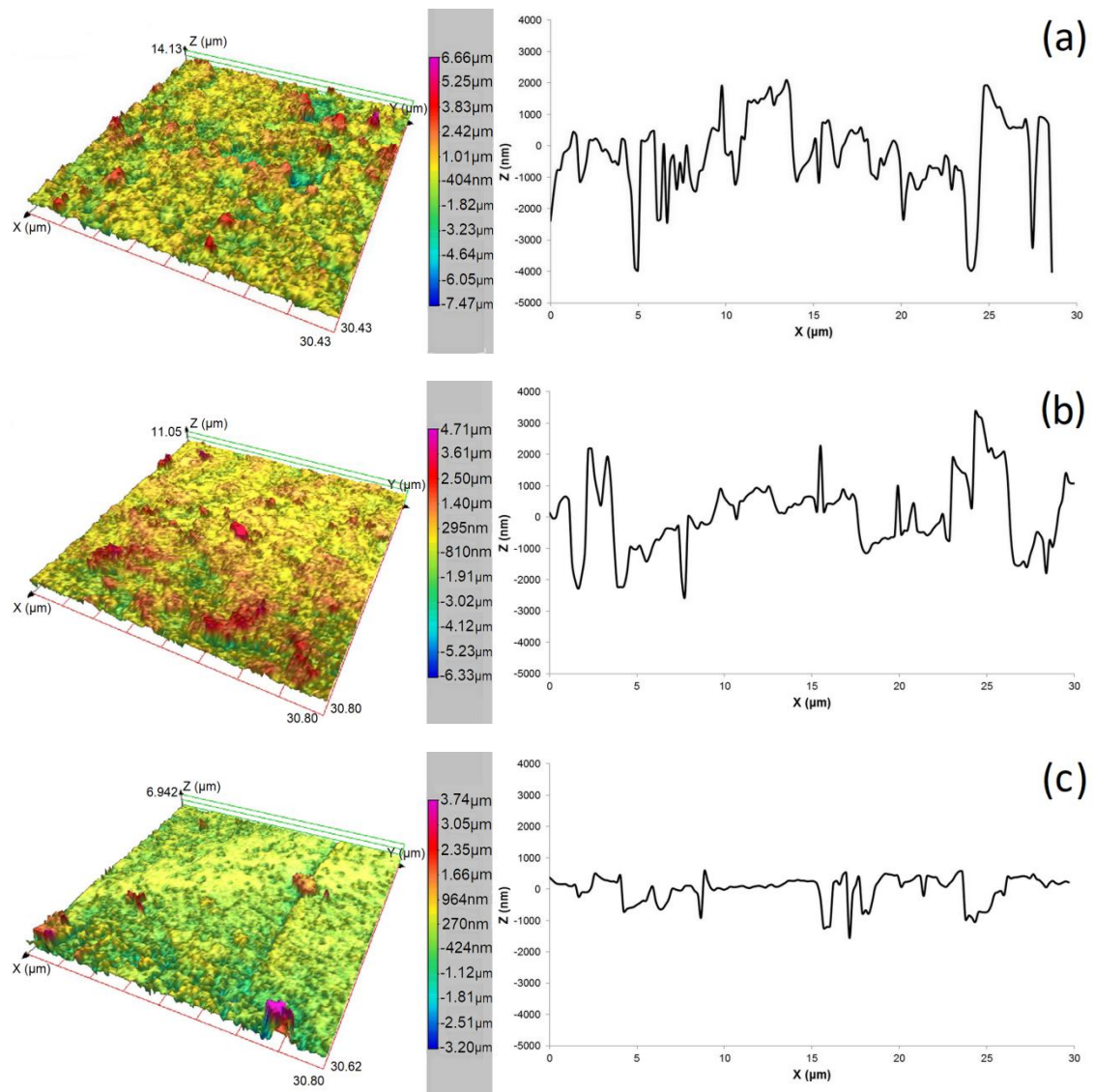
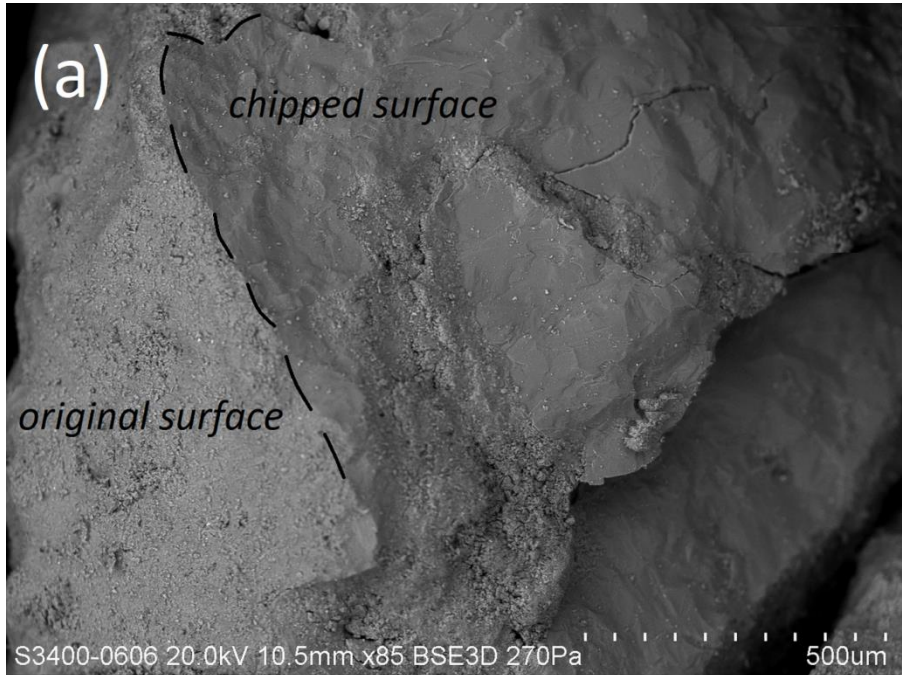


Fig. 10 3-D images of surfaces with different roughness and selected section profiles:
(a) $S_q=1300\text{nm}$, **(b)** $S_q=900\text{nm}$, **(c)** $S_q=450\text{nm}$



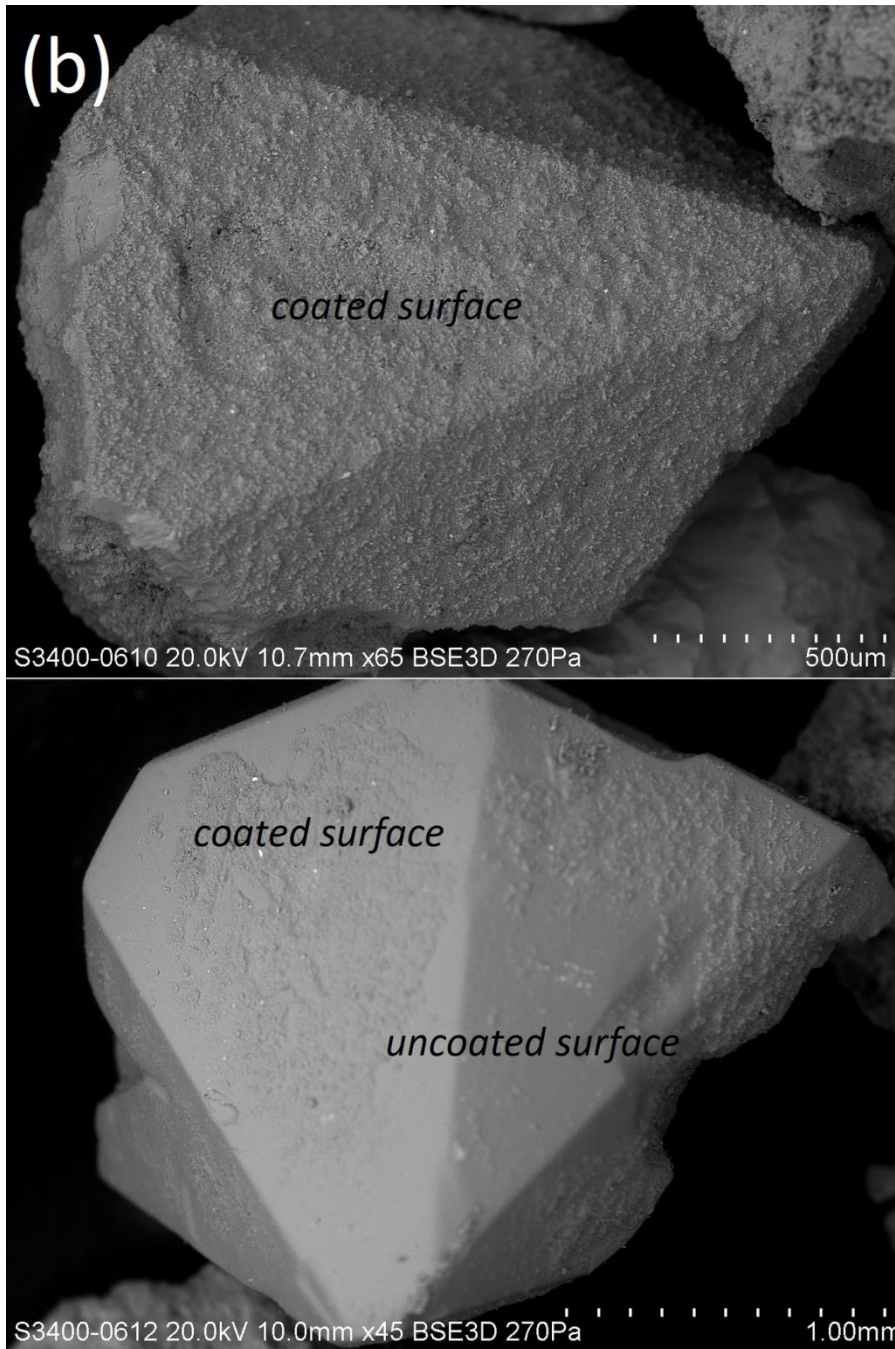


Fig. 11 SEM images of CDV particles after shearing: (a) particles showing an original and chipped surface, (b) quartz particles with coated and uncoated surfaces